

MAGNETIC LENSES FOR LOW ENERGY BEAM CHANNELS: COMPUTER SIMULATIONS AND EXPERIMENTAL MEASUREMENTS

S. Marghita¹, C. Matei², C. Oproiu², O. Marghita³, D. Toader²

¹ ICPE Electrostatica S.A., Bucharest

² National Institute for Lasers Plasma and Radiation Physics, Bucharest

³ Institute for Space Sciences, Bucharest

Abstract

Axial magnetic lenses are key elements of the beam channels in irradiation installations with low energy electrons. In order to achieve proper transport and focus of the electron beam in the target plane, careful computer design and execution of the lenses are needed. We present both the design and execution stages for an axial magnetic lens to be used with DIADYN, an effective laboratory installation for investigations of low energy electron beams. We also show experimental versus simulation results for one realized lens.

Keywords: low energy electrons, magnetic lens, computer simulation.

1. Introduction

The DIADYN installation was developed as a laboratory tool for conducting low energy (a few keV to a few 10 keV) electron beam studies, in functioning regimes similar to those used in applications (e.g. in material science). A successful application requires: (1) a good knowledge of the beam parameters, obtained by beam diagnosis, (2) a properly designed electron beam channel (EBC), as well as (3) a good understanding of the beam dynamics, i.e. of the beam transport through the EBC. When the conditions (1), (2), and (3) are satisfied, the precise tuning – according to the application – of the beam cross-section and energy density in the target plane becomes possible. In this paper we concentrate on the condition (2), by describing the work done so far to improve the EBC for DIADYN. Details on the beam diagnosis and dynamics – conditions (1) and (3) – as performed with DIADYN are given in [1] and [2], while an overview is also presented in [3].

In the present setup DIADYN (Fig. 1) includes a vacuum electron source, S, an EBC consisting of two axially symmetric magnetic lenses, L1, L2, and field free spaces, as well as a beam monitoring unit which includes two beam profile monitors, M1, M2, and a sliding Faraday cage. The beam propagation between the source and the target plane in the vacuum room, VR, is governed by the equation [4, 5]:

$$\frac{d^2R}{dz^2} + \frac{\eta B^2}{8U} R = \frac{1}{4\pi\epsilon_0\sqrt{2\eta}} \frac{I}{U^{3/2}} \frac{1}{R} + \frac{\epsilon^2}{R^3} \quad (1)$$

T_{spch} T_{em}

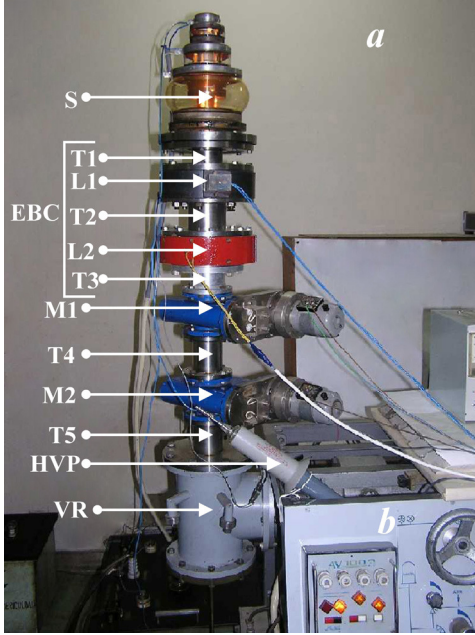


Fig. 1. The beam system (a), and part of the vacuum system (b), of the installation DIADYN. The beam system consists of: the electron source, **S**, the electron beam channel, **EBC**, the vacuum room, **VR**, and a monitoring unit. The EBC is made up of the magnetic lenses **L1**, **L2**, and the field free spaces **T1–T5**. The monitoring unit includes the beam profile monitors **M1**, **M2**, and a Faraday cage (not visible) which can slide along the EBC. Also shown is the high-voltage probe, **HVP**, used to measure the high-voltage applied to the source.

where R = root-mean-square (rms) beam radius, I = beam current, U = beam acceleration potential, ϵ = rms beam emittance, B = axial magnetic field, η = electron charge-to-mass ratio, ϵ_0 = dielectric constant. Equation (1) is valid only in paraxial approximation, therefore is critically important that this approximation is fulfilled. This requires the beam to be ‘thin’ compared to each lens (empirically, the beam radius should be less than about 1/3 of the lens radius). Since previous experiments showed that the beam grows large particularly within the lens L2, we started the optimization of the EBC with L2. The design and execution details of the new lens L2 are presented below.

2. EBC optimization: L2 design

The new lens L2 was designed to have better electrono-optical properties by: (1) enlarging the spool, which enables a larger paraxial region, and (2) enhancing the field confinement, through lateral flanges and soft iron polar pieces. A key tool used in the design phase was the simulation program FER1CH [6], based on a finite element code, which allows the calculation of the magnetic field for axially symmetric lenses. FER1CH requires information on the geometry of the lens, the magnetic properties of the materials, as well as the current (in ampere-turns) and area of the winding.

In order to find the best design solution for the lens L2, four alternative configurations have been modeled, as presented in Fig. 2:

- V1 has soft iron flanges at the edges. The spool welding belts are at the outer sides of the flanges.
- V1a is similar to V1, except for including soft iron polar pieces near the two interior faces of the spool. This adds a 20 x 4 mm air gap between the spool and the winding in the middle of the lens (see Fig. 5).
- V2 is similar to V1, but with the spool welding belts at the inner sides of the flanges.
- V2a is similar to V2, except for including soft iron polar pieces (same as V1a compared to V1).

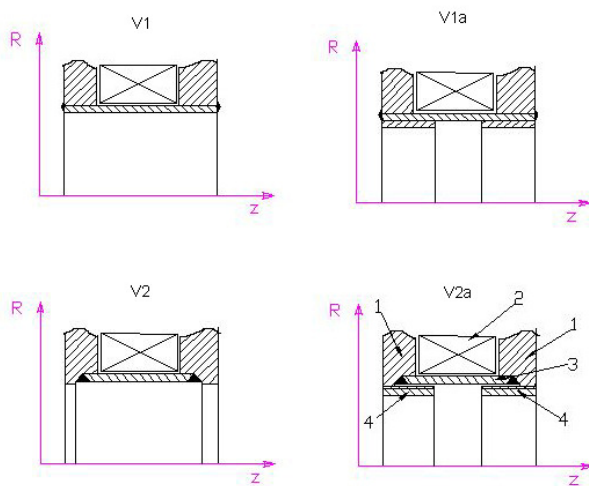


Fig. 2. Four possible design solutions for L2 (see text for details). The parts are indicated in the bottom right sketch:

- 1 – soft iron flanges
- 2 – coil winding
- 3 – stainless steel spool
- 4 – soft iron polar pieces

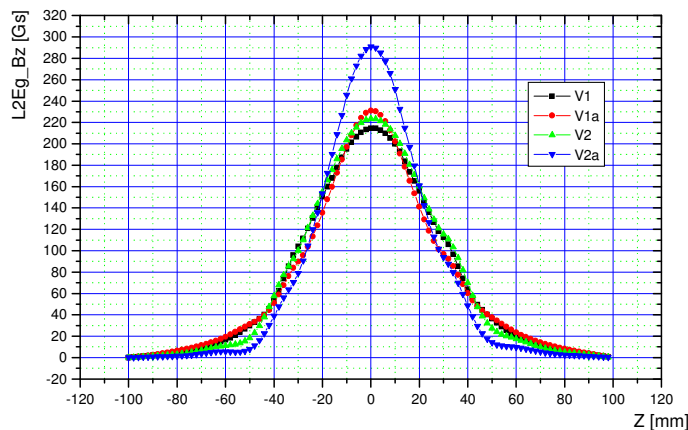


Fig. 3. Axial magnetic field corresponding to the four configurations from Fig. 3. The optimum field is seen to be obtained for the case V2a.

The axial magnetic field corresponding to the four configurations from Fig. 2 is presented in Fig. 3. The simulations were performed with a coil current of 1150 A-t (1 A by 1150 turns) and a coil surface of 11.56 cm². The configuration V2a provides the best field –

maximum value in the central plane of the lens, as well as steepest decrease towards the edges of the lense.

3. EBC optimization: L2 execution

The lens configuration selected for execution was V2a (Fig. 2), in agreement with the results of the design phase. Key stages of the execution phase are outlined by the photos in Fig 4, which show: (a) the spool after welding, with the welding belts at the inner sides of the flanges; (b) the flanges, with holes for fastening a soft iron cover; (c) the spool, after adding the polar pieces, facing, and boring.

The realized lens was slightly different as compared to the simulated lens. The wire used for the coil was thicker than assumed in the design simulations, which led to an increase of the winding surface from 11.56 cm^2 to 17.1 cm^2 . The final L2 configuration, used as input for FER1CH, is presented in Fig. 5 The corresponding magnetic field is shown in Fig. 6. For comparison, we show the magnetic field obtained both with and without polar pieces (Bzpp.sim and Bz.sim, respectively).

The photo in Fig. 7 shows the experimental arrangement used to measure the magnetic field along the L2 axis. The lens is equipped with a soft iron cover, acting as magnetic screen. Also visible are the power supply, an ampere-meter, and a gauss-meter with a Hall probe. As seen in Fig. 8, the agreement between the measured and simulated values of the magnetic field is very good, except for small differences due mainly to errors in positioning the Hall probe.



Fig. 4. Stages of L2 execution. Left: the spool after welding, with the welding belts at the inner sides of the flanges. Middle: the flanges, with holes for fastening a soft iron cover. Right: the spool, after adding the polar pieces, facing, and boring.

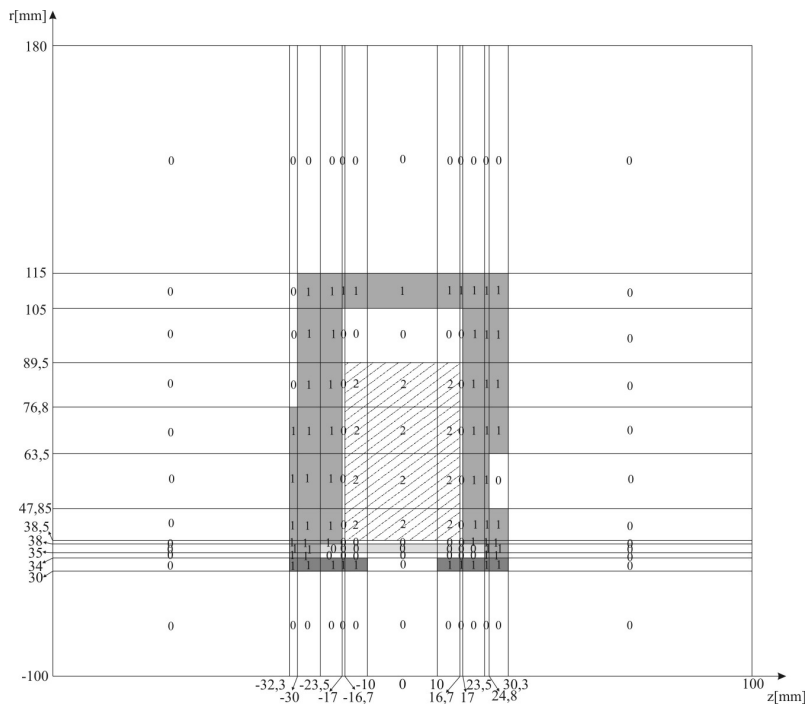


Fig. 5. Final L2 configuration, used as input for computer simulation. "0" (no filling), "1" (gray) and "2" (hatching) indicate, respectively, air (non-magnetic), soft iron, and the winding.

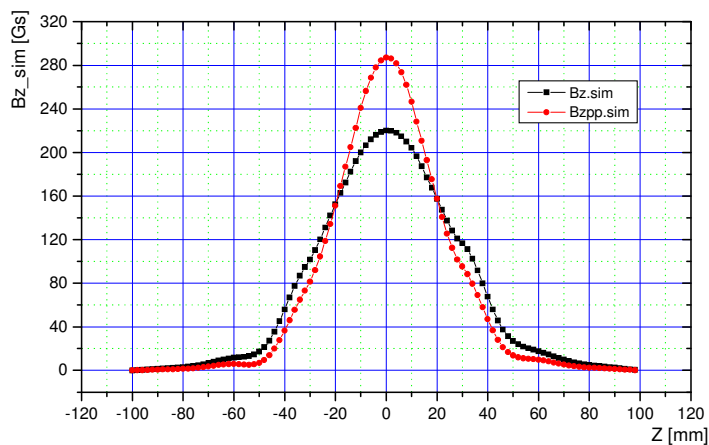


Fig. 6. Axial magnetic field, $B_{zpp}.sim$, obtained by simulation for the executed lens (Fig. 5). $B_z.sim$ is the field that would be obtained without polar pieces.

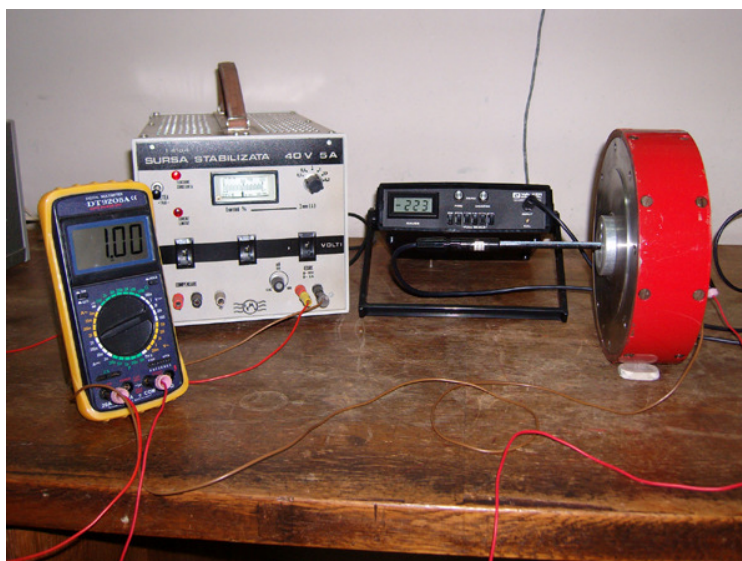


Fig. 7. Experimental arrangement used to measure the magnetic field along the L2 axis. The cover of the lens is a soft iron magnetic screen. Also visible are the power supply, an ampere-meter, and a gauss-meter with a Hall probe.

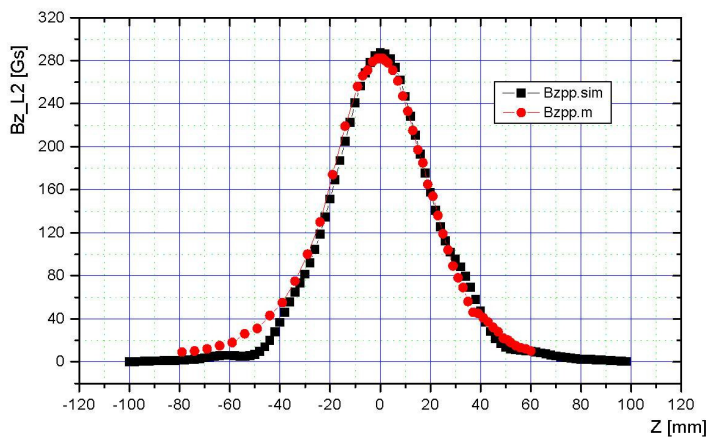


Fig. 8. Axial magnetic field simulated, $Bzpp.sim$, and measured, $Bzpp.m$.

Acknowledgment

The contribution of Emil Constantin to the execution of the experiments is thankfully acknowledged. The work was supported through the Project EGRETA, Program CEEEX 2006.

References

- [1] S. Marghitu, O. Marghitu, M. Rizea, C. Oproiu, and M. Vasiliu, *DIADYN - A Laboratory Setup for Experiments on Low Energy Electron Beams*, Proc. 8th Int. Conf. on Electron Beam Technologies, June 2006, Varna, Bulgaria, in *Electr. i Electronica*, No. 5–6, 276–280, 2006.
- [2] S. Marghitu, O. Marghitu, C. Oproiu, G. Marin, and Fl. Scarlat, *Diagnosis and dynamics in a simple low energy medium current electron beam channel*, *Nucl. Instr. Meth. B*, 217, 498–504, 2004.
- [3] S. Marghitu, O. Marghitu, C. Oproiu, D. Martin, and Fl. Scarlat, *On the design of low energy electron beam channels*, Proc. Phys. Conf. TIM03, November 2003, Timisoara, Romania, in *Analele Univ. de Vest, Timișoara*, Vol. XLIV, Științe Fizice, 197–202, 2003.
- [4] I.M. Kapchinskij and V.V. Vladimirkij, *Limitations of proton beam in strong focusing linear accelerator associated with the beam space charge*, Proc. Int. Conf. on High Energy Accelerators and Instrumentation, CERN, 274–288, 1959.
- [5] P. Ciuti, *On the equation defining the profile of non-relativistic beams with space charge forces and finite emittance*, *Nucl. Instr. Meth.*, 93, 295, 1971.
- [6] M. Rizea, *The mag. field calc. and the electron trajectory determination in computer aided design of unsaturated magnetic lenses*, *Rom. J. Phys.*, 37, 1031–1051, 1992.